A control design framework for wave energy devices

A control design framework for wave energy devices

Nicolás Faedo and John V. Ringwood

***Abstract*—This paper presents an integrated framework for the design of wave energy control systems, considering the totality of the design process as well as any ancillary functions required, such as model reduction, excitation force estimation, etc. In particular, we propose the moment-based mathematical framework as an integrated environment which allows a smooth transition between modelling and control activities, as well as providing a framework to consider optimal rejection of modelling errors or errors in excitation force estimation. The paper provides an overview of the framework, also containing an illustrative case study to demonstrate a likely pathway through the framework.**

***Index Terms*—Wave energy, Model reduction, Optimal control, Moments, Moment-matching**

I. Introduction

THE development of cost-competitive wave energy converter (WEC) technology is a challenging task. A key component in enhancing the technical and economic performance of a wave energy converter is an *energy-maximising control system* [1], which aims to utilise the capital infrastructure to the maximum economic advantage, while considering physical constraints and any impact of the control actions on the operational costs of the system. Somewhat similar to the diversity of wave energy devices themselves, a wide variety of control systems for wave energy devices also exists, from relatively simple structures (which try to implement some version of complex-conjugate control) [2] to those based on on-line numerical optimisation [3], [4]. Despite the range of potential controller choices, few consider the full WEC control process, from modelling to controller implementation.

We present the *moment-based* approach as an integrative framework for WEC controller design, underpinned by the efficient representation of system variables in terms of *moments* [5], [6]. Moments are connected to the input-output characteristics of the dynamical system under analysis, and provide a very specific parameterisation of the steady-state output response (provided it exists) of such a system. Such a parameterisation is given in terms of a so-called *signal generator* (see Section III), capable of representing a large class of 'basis' functions, including trigonometric polynomials (harmonic for control purposes), directly highlighting the inherent synergy between moments and the oscillating nature of the WEC harvesting process.

While different parameterisations, other than classical zero-order hold (*e.g.* [7]), and first-order hold [8], have already been utilised in the wave energy application [9]–[11] the proposed moment-based framework not only provides more freedom in terms of choice of basis functions (via an associated signal generator), but also has useful extensions to other control-related utilities for the wave energy application, including *model reduction*. In addition, it can be shown [12] that the general moment-based framework includes, for example, the pseudospectral approach of [9] as a special case.

A system theoretic approach to moment-matching was originally introduced by Astolfi [5], within the control systems literature, for model reduction, with a focus on maximal preservation of the steady-state response of the original system. One of the appealing characteristics of such a moment-based framework for model reduction is the degree to which it can handle both linear and nonlinear system models. Inspired by the flexibility of the moment-based framework, and its focus on steady-state responses, moment-based energy maximising WEC controllers were developed for both linear [13] and nonlinear [14] WEC models, representing the first moment-based *c*ontroller algorithms, irrespective of application area or control objective[1]. In addition, model reduction techniques, with specific focus on wave energy system requirements, have been developed, dealing with finite-order approximations to non-parametric hydrodynamic data (typically from Boundary Element Method (BEM) codes) [15]–[18] and more general nonlinear input/output descriptions [12], [19]. At the very least, these model reduction techniques establish a seamless link between hydrodynamic (and PTO) modelling and WEC controller design. Other aspects to the moment-based framework include extensions to deal with uncertainty (robust control) [20], [21] and arrays of WECs [22], [23], as well as receding-horizon implementations [24].

The paper is organised as follows: Section II gives an overview of the framework an its components and documents any aspects which remain to be completed, or where recourse must be made to aspects not covered by the framework *e.g.* hydrodynamic or PTO modelling.

Paper ID: XXXX. Track: XXXX.
This work was supported in part by Science Foundation Ireland under Grant 13/IA/1886 and the Marine Renewable Ireland Centre under Grant 12/RC/2302-2. This project has received funding from the European Union's Horizon 2020 research and innovation programme under the Marie Sklodowska-Curie grant agreement No 101024372. The results of this publication reflect only the author's view and the European Commission is not responsible for any use that may be made of the information it contains.

Nicolás Faedo is with the Marine Offshore Renewable Energy (MOREnergy) Lab., Department of Mechanical and Aerospace Engineering, Politecnico di Torino, Italy.

John V. Ringwood is with the Centre for Ocean Energy Research at Maynooth University, Ireland.

[1]Typically, in feedback control systems, the control objective is to minimise a tracking error, rather than energy maximisation.

In Section III, the mathematical basis for moment-based representations is outlined, along with various characteristics/standing assumptions of the moment-domain. Section IV establishes the starting point for the WEC design process (modelling) and examines model reduction requirements with a view to energy maximising control design. The WEC control problem is dealt with in Section V, addressing both linear and nonlinear designs, as well as WEC arrays. Sections VI and VII discuss moment-based controller versions suitable for explicitly dealing with modelling uncertainty, and receding-horizon controller implementations, respectively. Finally, following the case study of Section VIII, conclusions are drawn in Section IX.

II. Framework overview

An overview of the moment-based control design framework is given in Fig.1, where the 'path' followed in this paper to achieve energy-maximising moment-based control solutions is highlighted using green arrows. Note that different alternative paths could be taken, depicted in Fig. 1 using a dashed-red line. For instance, one could use moment-based model reduction to produce control-oriented models, which are suitable for a large class of optimal control procedures, according to the user's preference/experience.

In general, the framework is relatively complete, taking the user from the modelling stage (top of Fig. 1) to control implementation (bottom of Fig.1). Perhaps unsurprisingly, the moment-based framework does not address physical hydrodynamic modelling, which is firmly within the domain of hydrodynamic expertise, and a variety of hydrodynamic modelling approaches and codes are available [25], both in the realm of boundary element methods (BEMs) [26] or computational fluid dynamics (CFD) [27] and smoothed particle hydrodynamics (SPH) [28]. However, moment-based techniques can be useful in data-driven modelling, as outlined in Section IV.

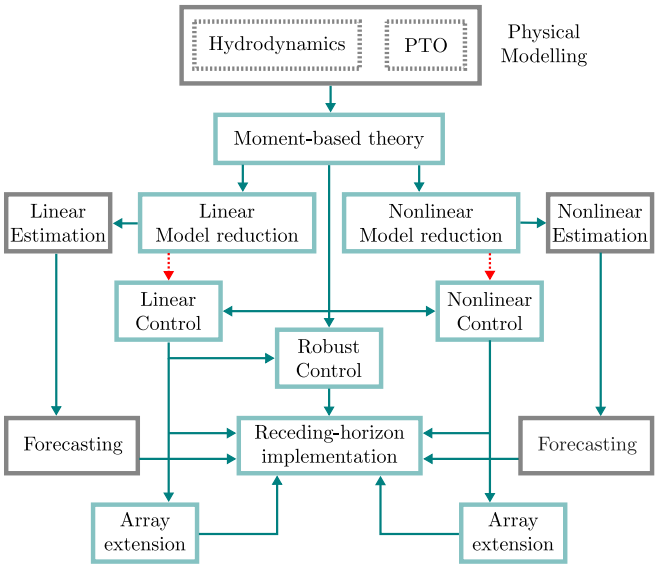

Fig. 1: Complete framework for WEC control design.

Ultimately, if control design is the objective, then a primary aim must be to get the system model into a form suitable for the application of model-based control/estimation design. While data-driven models can often be parameterised to suit model-based WEC control design needs, physics-based models (for both hydrodynamics and power take-off (PTO) components) rarely, if ever, do and some form of model manipulation or reduction is necessary. Within the moment-based framework, both linear and nonlinear model reduction tools have been developed, honing the models into a form suitable for control design.

On the control design side, the framework provides for linear and nonlinear WEC control design, array control design and robust control design, to deal with the inevitable modelling errors. However, robust control should not be seen as a panacea for all modelling problems; robust controllers are generally optimally conservative in their action, with the degree of conservatism related to the model uncertainty specified at the design stage, and are therefore no substitute for modelling excellence. Indeed, the specification of appropriate bounds on model uncertainty is, in itself, a nontrivial problem [29]. Within the moment-based framework, controller implementation is handled by a receding horizon scheme, using windowing functions and relying on updated estimates of wave excitation.

For excitation force estimation, required as an input to optimal non-causal WEC control schemes (see also Section V), in both single devices and arrays, the reader is referred to [30] and [31], respectively. The development of moment-based estimators and forecasters is a subject of current research, though some progress in this direction is reported in [32].

III. Moment-based theory: Key ingredients

This section briefly recalls some of the key concepts behind *moment-based* theory, as developed and discussed in, for instance, [5], [6]. In particular, we make special emphasis on the definition of *moments*, using a system-theoretic approach, and the set of 'key ingredients' required to formalise such a definition.

Suppose the dynamics associated with the WEC can be described in terms of a system Σ, defined, for $t \in \mathbb{R}^+$, by the set of differential equations

$$\Sigma : \{\dot{x} = f(x, f_e + f_{\text{PTO}}),\ y = h(x), \tag{1}$$

with f and h sufficiently smooth mappings defined in the neighborhood of the origin of Σ, with $f(0,0) = 0$ and $h(0) = 0$, and where x denotes the state-vector, f_e the wave excitation force, f_{PTO} the PTO (control) force, and y is the output of Σ. The first key ingredient of moment-based theory relies upon an implicit[2] description of the input mappings f_e and f_{PTO}: Let the so-called *signal generator* $\mathcal{G}$ be defined as

$$\mathcal{G} : \{\dot{\xi} = S\xi,\ f_e = L_e\xi,\ f_{\text{PTO}} = L_{\text{PTO}}\xi, \tag{2}$$

with $\xi(t)$, L_e, L_{PTO}, and S defined over real-valued spaces with appropriate dimensions. With the implicit

[2]Though not considered herein, an explicit description of the input mapping is also possible, see [12].

definition described in (2), we now consider the so-called *composite system*, *i.e.* the interconnection of (1) and (2), explicitly written as

$$\mathcal{G} \rightarrow \Sigma : \{\dot{\xi} = S\xi,\ \dot{x} = f(x, \mathcal{L}\xi),\ y = h(x), \tag{3}$$

with $\mathcal{L} = L_e + L_{\text{PTO}}$. The second key ingredient of moment-based theory, within the WEC application scenario, is closely related to the steady-state response output mapping of the composite system (3). In particular, the definition of moments, as proposed in [5], [6], has a strong connection with such a steady-state response (provided it exists). From now on, and with the objective of having a well-posed definition of moments, we adopt the set of assumptions described in Table I.

List of assumptions adopted:
1 - System Σ is *minimal*, *i.e.* observable and accessible.
2 - The origin of $\dot{x} = f(x, 0)$ is locally exponentially stable.
3 - The pair of matrices $(S, \mathcal{L})$ is observable.
4 - The pair of matrices $(S, \xi(0))$ is reachable.
5 - The matrix S is such that its eigenvalues are simple and with zero real part.

TABLE I: List of assumptions adopted.

Remark 1: None of the assumptions listed in Table I imply any loss of generality with respect to the practical application under scrutiny: Models for WEC systems are (or can be mapped to) minimal descriptions, which are locally exponentially stable (*i.e.* their linearisation about the zero equilibrium are asymptotically stable). Furthermore, since the implicit description (2) is user-defined, it is rather natural to construct (2) in such a way that all the modes of motion described by the dynamic matrix S are excited (reachability of $(S, \xi(0))$), and that the inputs generated are effectively observable (observability of $(S, \mathcal{L})$). Finally, the last assumption in Table I implies that the class of signals generated by (2) are those which can be written as linear combinations of $\{1, \sin, \cos\}$ type-terms, which is effectively consistent with the oscillating nature of the wave energy harvesting process (see also Section I).

The second key ingredient of moment-based theory now follows: Under the set of assumptions listed in Table I, there exists [5], [6] a unique mapping π, locally defined in a neighborhood Ξ of $\xi = 0$, which solves the nonlinear invariance equation

$$\frac{\partial \pi}{\partial \xi} S\xi = f(\pi(\xi), \mathcal{L}\xi), \tag{4}$$

for every $\xi \in \Xi$, and the steady-state response of the composite system (3) is $x_{\text{ss}}(t) = \pi(\xi(t))$, for any $x(0)$ and $\xi(0)$ sufficiently small. Based upon the implicit input description (2), and the steady-state manifold equation (4), we can now formalise the definition of moment: The mapping $h \circ \pi$, with π solution of the invariance equation (4), is the *moment* of system (1) at the signal generator (2).

Remark 2: Under the assumptions listed in Table I, the moment of system (1) at the signal generator (2) computed along a particular trajectory $\xi(t)$ *coincides* with the (well-defined) steady-state output response of the composite system (3), *i.e.* $y_{\text{ss}}(t) = h(\pi(t))$.

Remark 3: In the special case where system (1) is assumed to be fully linear, *i.e.*

$$\Sigma : \{\dot{x} = Ax + B(f_e + f_{\text{PTO}}),\ y = Cx, \tag{5}$$

the mapping π can always be written as $\pi(\xi) = \Pi\xi$, with Π solution of the Sylvester equation $\Pi S - A\Pi = B\mathcal{L}$ (*i.e.* the invariance equation (4) for the linear system (5)), and hence the moment at the signal generator (2) is simply given as the matrix product $C\Pi$, with $y_{\text{ss}}(t) = C\Pi\xi(t)$.

It should be clear at this point that moments provide a very specific parameterisation of the steady-state output response of system (1), driven by the set of inputs generated by (2). We show, throughout this paper, that such a parameterisation can be extremely useful within the WEC community, being fundamental to provide tailored solutions to two key problems: *Model reduction* and *energy-maximising optimal control*.

IV. Modelling and Model Reduction

For model-based control design, it is essential that the control objective is considered at an early stage, so that this ultimate objective colours the design process even at the modelling stage. This streamlines the process from modelling through to control design, including any model reduction steps necessary en route. One important aspect of model-based control design is the need to have a representative hydrodynamic model which covers the operational space of the *controlled system*, as clearly illustrated in [33], [34]. Typically, for many WEC devices, the extent of the controlled operational space leads to nonlinear hydrodynamic behaviour, due to increases in wetted surface and viscous drag. While a good model of the power take-off (PTO) system is also important, scale and operational range issues are not as challenging as for the hydrodynamics, though physical PTO system constraints on force, displacement, and possibly velocity, are important to the control problem definition (further detailed in Section V).

Moments, as defined in Section III, are key elements for a powerful state-of-the-art model reduction framework: the family of so-called *moment-matching*-based model reduction. This set of techniques consists of the interpolation of the steady-state response of the output of the system Σ to be reduced: a reduced order model by moment-matching $\tilde{\Sigma}$ is such that its steady-state output response *matches* the steady-state output response of the associated target system (1). Furthemore, we show that the user has full control over the complexity of the moment-based approximating model, even in the nonlinear case, highlighting the versatility of this framework to trade-off complexity vs. accuracy.

Remark 4: We consider here moment-matching-based model reduction for structures which respond to physical laws: One starts with a defined operator (*i.e.* Σ in (1)), and attempts to reduce this model into a tractable form for control/estimation purposes. Though not explicitly discussed here, one could also consider either CFD codes or real experimentation to construct a set of representative system outputs, for a specific class of inputs, to later construct control-oriented representations which describe the dynamics of a given WEC, using data-driven moment-matching (see [35]).

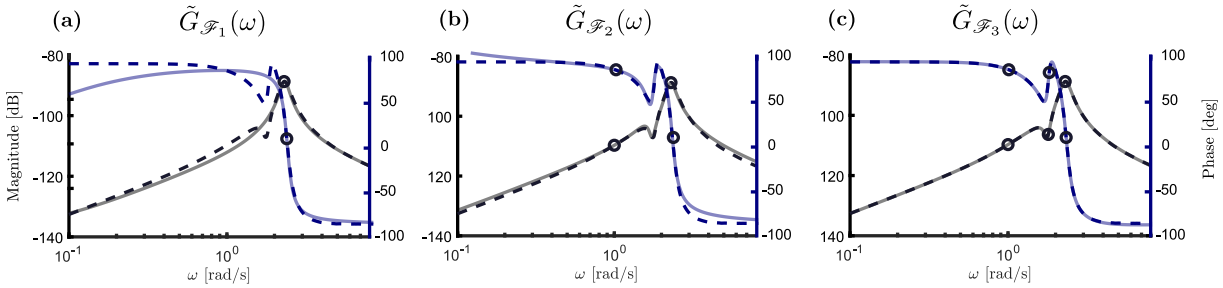

Fig. 2: Bode plot for the moment-based reduced models (toroidal device). In particular, **(a)**, **(b)** and **(c)**, show the frequency response of the moment-based systems (solid) $\tilde{\Sigma}_{\mathscr{F}_1}$, $\tilde{\Sigma}_{\mathscr{F}_2}$ and $\tilde{\Sigma}_{\mathscr{F}_3}$, *i.e.* $\tilde{G}_{\mathscr{F}_1}$, $\tilde{G}_{\mathscr{F}_2}$ and $\tilde{G}_{\mathscr{F}_3}$, respectively. The target frequency response $G(\omega)$ is depicted in all plots with a dashed line. Fig. adapted from [36].

A. Finite order linear parameterisation

Under linear potential flow theory [37], hydrodynamic models for WEC systems can be generally represented in terms of the feedback interconnection of two different subsystems, *i.e.* Σ_I and Σ_r, as in Fig. 3. In particular, System Σ_I represents inertial effects, while system Σ_r represents fluid memory effects that incorporate the energy dissipation due to waves radiated as a consequence of the motion of the structure. Note that this representation is very general, and includes both single and multiple degree-of-freedom (DoF) devices, as well as WEC arrays.

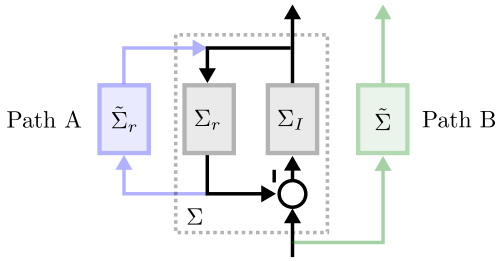

Fig. 3: Schematic of linear model reduction.

While system Σ_I depends upon a finite number of fixed and static system parameters (*e.g.* mass and hydrostatic stiffness of the device), Σ_r is virtually always built upon a specific impulse response function [37], characterised by means of hydrodynamic codes in terms of a finite number of data-points in the frequency-domain. In other words, the output response of Σ_r needs to be computed in terms of a specific *convolution* operation. The mere presence of this non-parametric convolution term implies both a representative and a computational drawback for a variety of applications, including WEC control/estimation procedures.

Model reduction techniques can be used to parameterise this operator (denoted as Path A in Fig. 3), commonly in terms of a state-space representation, which should ideally retain the underlying physical properties that characterise the WEC process. In particular, a moment-matching-based solution has been initially proposed in [15], for single-DoF devices. This has been later extended to multi-DoF systems in [16], and WEC arrays in [17], [18]. Furthermore, note that a critical comparison between this moment-based approach, and a set of well-established parameterisation techniques in the wave energy field, can be found in [38].

If the system is *linear* (as in this case), the steady-state output response is *fully characterised* by its associated frequency-domain mapping. In other words, moments are in a one-to-one relation with the frequency-response associated with the target system: *Matching moments directly implies interpolation of the target frequency-response at a finite number of points, i.e.* frequencies. Furthermore, as shown in [38], [39], essential physical properties of the device can be retained by (or enforced on) the reduced order model by moment-matching as a result of this frequency interpolation feature, such as internal stability, passivity, and zero dynamics.

Remark 5: Perhaps unsurprisingly, the interpolation frequencies are the eigenvalues of the dynamic matrix S in (2). One can achieve *exact* interpolation at a (user-selected) set of finite number of points by simply shaping $\lambda(S)$ accordingly. Note that, if a frequency $\omega \in \mathbb{R}$ is selected, then both $\pm j\omega$ need to be chosen as eigenvalues of S, so as to keep system (2) defined over $\mathbb{R}$. This automatically implies that the dimension (order) of the resulting reduced model is *twice* the number of interpolation points, for each DoF (and WEC) considered in the parameterisation [17], [18].

Another potential path, to achieve a parametric representation of WEC models, is to apply a moment-matching reduction procedure to the input-output system Σ directly, *i.e.* using the frequency response of the closed-loop behaviour in Fig. 3 (Path B).

1) Case study: We now present a case study based on a toroidal geometry (floater), which constitutes one of the main components of devices such as, for instance, the Ocean Power Technologies (OPT) point absorber WEC [40]. For simplicity of presentation, the geometry is assumed to be constrained to move in heave (translational motion), which is effectively the DoF from where energy is absorbed in [40]. We discuss moment-based reduced models for the input-output dynamics (force-to-velocity) case only (Path B in Fig. 3), for economy of space. An analogous procedure can be carried out for the radiation system straightforwardly.

A sensible selection of the set of interpolation points (frequencies) can be performed by analysing the gain of the target frequency response, herein termed $G(\omega)$, and selecting points that characterise dynamically important features of the WEC. A sensible selection includes the resonant frequency of the device under consideration. Note that this is, effectively, the frequency where the maximum amplification occurs, *i.e.* the

frequency characterising the $\mathscr{H}_\infty$-norm of the WEC system. Based on the previous discussion, different sets of interpolation frequencies are chosen as follows: $\mathscr{F}_1 = \{2.3\}$, $\mathscr{F}_2 = \{1, 2.3\}$, and $\mathscr{F}_3 = \{1, 1.8, 2.3\}$. Note that $\mathscr{F}_i \subset \mathscr{F}_j$ for $i < j$. As can be appreciated from Fig. 2, the set $\mathscr{F}_1$ already includes a key interpolation point, *i.e.* the resonant frequency associated with the DoF under analysis. The set $\mathscr{F}_2$ additionally includes a low-frequency component, while the set $\mathscr{F}_3$ further expands $\mathscr{F}_2$ by including a mid-frequency component.

Fig. 2 presents the Bode plot, for both the target frequency response $G(\omega)$ (dashed), and the approximating frequency response mappings (solid) $\tilde{G}_{\mathscr{F}_1}(\omega)$ in **(a)**, $\tilde{G}_{\mathscr{F}_2}(\omega)$ in **(b)**, and $\tilde{G}_{\mathscr{F}_3}(\omega)$ in **(c)** (corresponding with $\mathscr{F}_1$, $\mathscr{F}_2$, and $\mathscr{F}_3$, respectively). As expected by the theoretical foundations of this moment-based strategy, the approximating models have *exactly* the same frequency-domain behaviour as the target model $G(\omega)$, for each element of the corresponding interpolation set $\mathscr{F}$, with a clear decrease in the overall approximation error from system $\tilde{G}_{\mathscr{F}_1}$ towards $\tilde{G}_{\mathscr{F}_3}$.

B. Nonlinear model reduction

If we go beyond linear potential flow theory, the equation of motion describing the WEC system Σ is not only non-parametric, but can also present complex nonlinear effects, which can render control and/or state-estimation strategies unsuitable for realistic applications: There is a limit for both the analytical complexity for which a controller/estimator can be effectively synthesised, and handled in real-time.

The nonlinear moment-based framework, recalled in Section III, has been recently shown to be a valuable tool for model reduction of nonlinear WECs in [19], given the inherent preservation of steady-state response characteristics. In particular, given that the computation of a reduced model by moment-matching for nonlinear systems relies on the availability of a closed-form solution of the nonlinear partial differential equation (4), [19] proposes an approximation for the nonlinear moment, with guarantees of uniform convergence.

The family of nonlinear models reduced by moment-matching proposed in [19] is inherently parametric (given specifically in state-space form), and input-to-state *linear*, with any nonlinear behaviour confined to the output mapping only (*i.e.* a Wiener model). The linear input-to-state model is characterised in terms of a set of (user-supplied) dynamically relevant frequencies $\mathscr{F}$, analogously to the linear case in Section IV-A. Moreover, given the nature of the Galerkin-like method proposed to approximate the corresponding moment, the user can manipulate the degree of complexity of this nonlinear output mapping, which is defined via polynomial functions of the state-vector of the associated signal generator (2), *i.e.* ξ, with a user-defined maximum degree N_p, hence having full control of the underlying characteristics of the reduced structure. Naturally, a large value for N_p automatically implies a high degree of accuracy, at the expense of an increase in complexity, and vice versa.

1) Case study: To highlight the main features of the nonlinear moment-based model reduction framework, an array of two identical spherical heaving point absorber WECs is considered, each device with a radius of 2.5 [m], and a distance between devices set to 5 [m] (see [19] for further detail). The input-output model not only is non-parametric, but the following mapping f_{nl}, characterising the nonlinear effects for this WEC system, is considered: $f_{nl}(z, \dot{z}) = \begin{bmatrix} f_{re}^{\text{nl}}(z_1) + f_v(\dot{z}_1) & f_{re}^{\text{nl}}(z_2) + f_v(\dot{z}_2) \end{bmatrix}^\intercal$ where $f_{re}^{\text{nl}}(z) = \alpha_1 z^3$ and $f_v(\dot{z}) = \alpha_2 \dot{z}|\dot{z}|$ represent nonlinear hydrostatic restoring, and viscous drag effects, respectively, and where $z_1 : \mathbb{R}^+ \to \mathbb{R}$ and $z_2 : \mathbb{R}^+ \to \mathbb{R}$ denote the displacement of device 1 and 2, accordingly. The specific values for $\{\alpha_1, \alpha_2\}$ can be found in [19].

The numerical generation of the (irregular) input waves is fully characterised by a JONSWAP spectrum with $\bar{H}_w = 2$ [m], $\bar{T}_w = 8$ [s] and peak enhancement factor is set to $\gamma = 3.3$. In addition, the set of frequencies considerd to characterise the input-to-state dynamics of the reduced model is $\mathscr{F} = \{0.8, 2\}$. With this selection of frequencies, the order (dimension) of the reduced model by moment-matching is $2f = 4$.

Remark 6: As in Section IV-A, the selection of the set $\mathscr{F}$ is not arbitrary: 0.8 [rad/s] represents the frequency corresponding with the peak characterising the input spectral density function, while 2 [rad/s] is the frequency characterising the $\mathscr{H}_\infty$-norm of the Jacobian linearisation of the WEC system, *i.e.* the resonant frequency corresponding to heave motion (see [19]).

Finally, the nonlinear output map characterising the reduced model (which effectively results from the Galerkin-based approximation of the corresponding nonlinear moment), is given in terms of a fifth-order polynomial surface in ξ, *i.e.* $N_p = 5$.

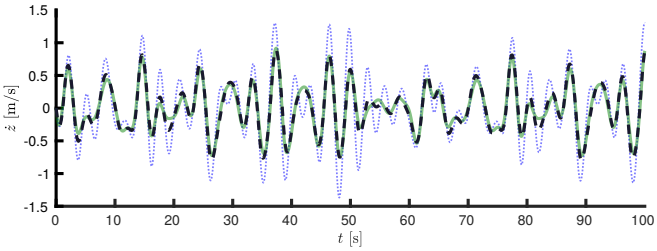

Fig. 4: Output of the reduced order model by moment-matching (solid) and target motion (dashed), for a randomly generated sea-state realisation. The output of the Jacobian linearisation about the origin is also shown, using a dotted blue line. Fig. adapted from [19].

To briefly assess the resulting reduced order model by moment-matching, Fig. 4 presents results for a particular (randomly generated) sea state realisation. As can be directly appreciated from Fig. 4, the output of the reduced order model by moment-matching (solid) is effectively able to approximate the target output (dashed), even during the transient period. For the benefit of the reader, the output corresponding with the (non-parametric) Jacobian linearisation of the WEC model about the origin, is also presented, using a dotted line. A significant overprediction of velocity can be appreciated by the linear model, potentially leading to

an overprediction of power production, which is the core variable in any energy-maximising controller. The normalised mean average percentage error for 100 [s] of simulation time (as shown in Fig. 4), is $\approx 4.6\%$ for the nonlinear reduced model computed in this section, vs. $\approx 40\%$ for the case of the Jacobian linearisation.

V. Control of WECs and WEC arrays

WEC optimal control design entails an *energy-maximisation* criterion, where the objective is to maximise the absorbed energy from ocean waves over a time interval $\mathcal{T} \subset \mathbb{R}^+$, which can be cast as an optimal control problem (OCP), with an *objective function* $\mathcal{J}$

$$\mathcal{J}(f_{\text{PTO}}) = \frac{1}{T}\int_{\mathcal{T}} f_{\text{PTO}}(\tau)\dot{z}(\tau)d\tau, \tag{6}$$

where f_{PTO} and z denote the control (PTO) force (to be optimally designed), and the displacement of the WEC, respectively. Given that the unconstrained energy-maximising optimal control law often implies unrealistic device motion and excessively high PTO (control) forces (see [2], [3]), constraints on both the displacement and velocity of the WEC, z and $\dot{z}$, and the exerted control force f_{PTO}, have to be considered within the optimal control design, which can be compactly written as

$$\mathscr{C} : \Big\{ |z| \leq Z_{\max},\, |\dot{z}| \leq \dot{Z}_{\max},\, |f_{\text{PTO}}| \leq F_{\max}, \tag{7}$$

with $t \in \mathcal{T}$, and where $\Big\{Z_{\max}, \dot{Z}_{\max}, F_{\max}\Big\} \subset \mathbb{R}^+$.

Given the control objective function defined in (6), and the set of state and input constraints defined in (7), the constrained energy-maximising OCP is

$$\begin{aligned} f_{\text{PTO}}^{\text{opt}} &= \arg\max_{f_{\text{PTO}}} \ \mathcal{J}(f_{\text{PTO}}), \\ &\text{s.t.: WEC dynamics } \Sigma \text{ \& Constraint set } \mathscr{C}, \end{aligned} \tag{8}$$

where system Σ describes the dynamic motion of the device, in the form of (1).

Remark 7: In order to solve the OCP defined in (8), full knowledge of the wave excitation force is required for the time-interval $\mathcal{T}$, *i.e.* solving (8) implicitly requires *instantaneous* and *future* values of wave excitation, computed via estimation and forecasting strategies, respectively. The reader is referred to [30], [31] for further detail on input-unknown estimation and forecasting techniques applied within the WEC field.

The underpinning idea of the moment-based optimal control framework, initially proposed for linear systems in [13], is to solve the OCP (8) via parameterisation of the steady-state output response of the WEC system in terms of moments. In particular [13] shows that, besides being a powerful model reduction tool (as demonstrated in the Section IV), the parameterisation of the steady-state response of the WEC system in terms of moments (*i.e.* in terms of the solution of a specific invariant equation, see Section III), can be explicitly used to transcribe the (infinite-dimensional) energy-maximising control problem (8) to a finite-dimensional optimisation program. In other words, the main idea behind moment-based optimal control is to substitute the WEC dynamic constraint in (8) by the parameterisation of the WEC system in terms of moments, explicitly using its steady-state output behaviour to solve for the corresponding optimal control input, in terms of a suitably specified signal generator (2) (further detail in Section V-A). Furthermore, unlike the majority of the model-based energy-maximising control strategies reported for WECs (see [3]), this moment-based strategy *does not require a-priori* parametric approximation (*i.e.* model reduction) of Σ_r, but actually provides an analytical description of the radiation convolution in the moment-domain, further reducing the associated computational burden.

A. Linear case

Within the linear moment-based optimal control framework, the energy-maximising OCP can be mapped into a *strictly concave* quadratic program (QP), guaranteeing a unique solution for the energy-maximising control objective, subject to both state and input constraints. This has a strong impact on the practical viability of the moment-based approach, facilitating the utilisation of state-of-the-art QP solvers (see [41]), providing a computationally efficient energy-maximising framework.

In particular, given the harmonic nature of ocean waves (see [42]), both excitation force and control inputs are expressed in terms of a signal generator as in (2), with dynamic matrix S such that $\lambda(S) = \{\pm p\omega_0\}_{p=1}^{N_h}$, where ω_0 is the so-called *fundamental frequency* associated with the input variables. In other words, the signal generator is chosen such that the moments of the WEC system are computed at a finite number of N_h harmonics of the fundamental frequency ω_0, hence characterising the steady-state response of the WEC at these harmonic frequencies. Note that the associated *fundamental period* is simply given by $T_0 = 2\pi/\omega_0$. With this specific selection of signal generator, the OCP (8), with $T = T_0$, can be mapped to a *strictly concave* QP problem, *i.e.* with a problem with a structure:

$$\begin{aligned} L_{\text{PTO}}^{\text{opt}} &= \arg\max_{L_{\text{PTO}} \in \mathbb{R}^{2N_h}} \mathcal{QP}(L_{\text{PTO}}), \\ &\text{s.t.: } \mathcal{I}L_{\text{PTO}} \leq \mathcal{O}, \end{aligned} \tag{9}$$

where the optimal force is $f_{\text{PTO}}^{\text{opt}} = L_{\text{PTO}}^{\text{opt}}\xi$, with ξ the state-vector of the associated signal generator, and the set of *linear inequalities* in $\{\mathcal{I}, \mathcal{O}\}$ represent the moment-based parameterisation of the set of state and input constraints in (7). The reader is referred to [13] for the analytical definition of the matrices involved in (9).

Remark 8: Unlike, for instance, MPC, concavity of (9) is guaranteed *without* the need for adding regularisation terms, which can effectively bias the energy-maximising objective. Strict concavity of (9) is a consequence of the synergy between moments and the WEC harvesting process: Due to its oscillating nature, the parameterisation of the state-variables in terms of moments retains fundamental input-output properties of the WEC model, such as passivity. This is, indeed, exactly what guarantees existence of a unique global solution in (9).

B. Nonlinear case

The paper [14] presents an energy-maximising control strategy for WECs subject to *nonlinear* dynamics. In

particular, a method to map the objective function (and system variables) to a finite-dimensional nonlinear program (NP), is proposed, which can be efficiently solved using state-of-the-art NP solvers [41].

In particular, since, for nonlinear systems, the computation of the associated moment depends upon the nonlinear invariance equation (4), an approximation framework for π is presented in [14], tailored for the optimal control scenario. Such an approximation strategy relies upon an 'extension' of the signal generator utilised in the linear case of Section V-A: A higher number of harmonics $\bar{N}_h > N_h$, is considered to construct $\lambda(S)$, giving origin to the so-called *extended signal generator*, with state-vector denoted as $\bar{\xi}$. Such a generator is achieved via a set of suitably defined inclusion mappings, such that $\text{span}\{\xi_i\} \subset \text{span}\{\bar{\xi}_i\}$, *i.e.* the function space generated by the elements of the state-vector of the signal generator utilised in Section V-A is effectively 'expanded' to a higher dimensional structure, generated in terms of a higher number of harmonics of the fundamental frequency ω_0. The approximated moment is then computed by a Galerkin-like procedure, *i.e.* by projecting π onto the space spanned by the extended state-vector $\bar{\xi}$ (see also [12]).

Summarising, the procedure proposed in [14] maps the OCP (8) for nonlinear WEC systems, to a finite-dimensional NP with the following structure:

$$\begin{aligned} &\bar{L}_{\text{PTO}}^{\text{opt}} = \arg \max_{\bar{L}_{\text{PTO}} \in \mathbb{R}^{2\bar{N}_h}} \mathcal{QP}(\bar{L}_{\text{PTO}}) + \mathcal{B}(\bar{L}_{\text{PTO}}), \\ &\text{s.t.: } \bar{\mathcal{I}}(\bar{L}_{\text{PTO}}) \leq \bar{\mathcal{O}}(\bar{L}_{\text{PTO}}), \end{aligned} \tag{10}$$

where the optimal force is $f_{\text{PTO}}^{\text{opt}} = \bar{L}_{\text{PTO}}^{\text{opt}} \bar{\xi}$, with $\bar{\xi}$ the state-vector of the associated *extended* signal generator, and where the mappings $\{\bar{\mathcal{I}}, \bar{\mathcal{O}}\}$ represent the set of state and input constraints defined in (7).

Remark 9: Due to the synergy between moments and the WEC harvesting process (see also Remark 8), the finite-dimensional moment-based NP presented in (10) is composed of the sum of a *concave quadratic term*, *i.e.* $\mathcal{QP}(\bar{L}_{\text{PTO}})$, and a bounded perturbation $\mathcal{B}(\bar{L}_{\text{PTO}})$. In other words, the mapped objective in (10) belongs to a family of approximately concave mappings (so-called outer Γ-concave [43] functions), from where existence of a global energy-maximising solution can be guaranteed, under *mild* assumptions (see [14]). Furthermore, similarly to the case of concave functions, where each local solution is also global, explicit conditions to determine whether a local energy-maximising solution is a global maximiser for the OCP, can be derived, having strong practical value when solving the associated NP.

C. WEC arrays

As detailed in [22], [23], the case of WEC arrays can be dealt with analogously to Sections V-A (linear WEC) and V-B (nonlinear WEC), with a suitable re-definition of the associated signal generators. In particular, each respective signal generator needs to be *augmented* by the number of devices in the array N_d. This can be achieved straightforwardly, by 'replacing' each corresponding dynamic matrix S by its augmented counterpart, *i.e.* by $\mathbb{I}_{N_d} \otimes S$. This naturally implies that the finite-dimensional moment-based programs presented in (9) and (10), will be now carried over $\mathbb{R}^{2N_h N_d}$ and $\mathbb{R}^{2\bar{N}_h N_d}$, respectively, *i.e.* the optimisation space is 'augmented' by the number of devices N_d in both cases. This is done *without losing the benefits of the moment-based optimal control approach*: For linear arrays, the control problem is still strictly concave, while for nonlinear systems, strict outer Γ-concavity is retained, hence also always admitting a globally optimal energy-maximising solution (*i.e.* computationally tractable).

VI. Robustifying the control solution

The presence of *system uncertainty* is ubiquitous in hydrodynamic modelling. By way of example, some parameters of the WEC hydrodynamic model can vary significantly due to the change in the relative motion of the device [44], or simply due to unmodelled dynamics, not captured by the (nominal) WEC model. System uncertainty is not the only source of error inherently present in the WEC energy-maximising optimal control problem: Given that the wave excitation force, which is a key variable in the OCP (8), is virtually always approximated by means of unknown-input estimation (instantaneous values) and forecasting (future values) techniques, *input uncertainty* is also ubiquitous.

Moment-based solutions for the case of system and input uncertainties are presented in [20] and [21], respectively. Both techniques are based upon a suitable moment-based characterisation for the uncertainty, taking into consideration an appropriate uncertainty set, written in terms of a convex polytope defined over a real vector space. To this end, the concept of moments is combined with the robust optimisation principles considered in [45], by proposing a *worst-case performance* (WCP) approach. Necessary and sufficient conditions on the uncertainty polytope can be explicitly derived, so that the moment-based robust optimal control framework *always admits a global energy-maximising solution*, preserving all the appealing characteristics of the (nominal) strategy described in Section V-A.

To be more precise, it is assumed that a nominal WEC system Σ^0 and signal generator $\mathcal{G}^0$ are known, and that the actual system $\Sigma^\star$, and generator $\mathcal{G}^\star$, are known to lie within a set of *convex* polytopes, denoted as $\mathcal{P}_\text{s}$ (system) and $\mathcal{P}_\text{i}$ (input), respectively. This is shematically depicted in Fig. 5, where the elements inside each respective polytope are characterised by the so-called uncertainty vector δ.

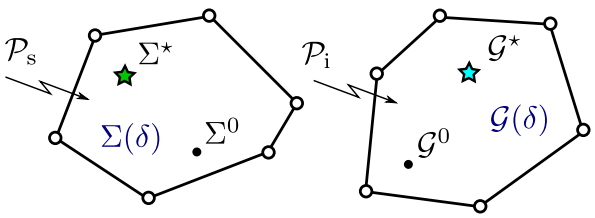

Fig. 5: Schematic representation of uncertainty polytopes for both system (left) and input (right) uncertainty.

With such a characterisation of the uncertainty, the moment-domain optimisation problems recalled in

Section V-A can be re-formulated based on an OCP approach. To economise space, suppose $\tilde{\mathcal{J}}$ denotes the linear moment-based objective function (as in Section V-A), for a given number of harmonics in the corresponding signal generator with state-vector $\tilde{\xi}$. Let $V_{\mathcal{P}}$ denote the set of vertices associated with either $\mathcal{P}_{\rm s}$ or $\mathcal{P}_{\rm i}$. The robust moment-based optimisation problem can be then formulated, for either system or input uncertainty, in terms of the following structure:

$$\begin{aligned} &L_{\rm PTO}^{\rm rob} = \arg\max_{\tilde{L}_{\rm PTO}} \ \arg\min_{\delta\in V_{\mathcal{P}}} \tilde{\mathcal{J}}(\tilde{L}_{\rm PTO},\delta), \\ &\text{s.t.: } \tilde{\mathcal{I}}(\tilde{L}_{\rm PTO},\delta) \leq \tilde{\mathcal{O}}(\tilde{L}_{\rm PTO},\delta),\ \forall \delta \in V_{\mathcal{P}}, \end{aligned} \tag{11}$$

where the robust optimal control force can be computed as $f_{\rm PTO}^{\rm rob} = L_{\rm PTO}^{\rm rob}\tilde{\xi}$, with $\tilde{\xi}$ the state-vector of the associated signal generator, and where the mappings $\{\tilde{\mathcal{I}},\tilde{\mathcal{O}}\}$ represent the set of state and input constraints defined in (7), as a function of the uncertainty vector δ. The problem defined via (11) computes the *worst-case scenario* for the moment-based energy-maximising problem, with respect to *every possible uncertainty vector* δ, lying inside the corresponding polytope $\mathcal{P}$.

Remark 10: As a direct consequence of the existence of a unique globally optimal energy-maximising solution (see Section V-A), and the definition of the moment-based uncertainty in terms of a convex polytope, it is sufficient to solve the robust formulation presented in (11) *only for the elements of the finite set of vertices* $V_{\mathcal{P}}$, hence (11) being *computationally tractable*. Furthermore, guaranteeing constraint satisfaction at every point of the set of vertices V_δ, automatically ensures constraint satisfaction *for every possible uncertainty* $\delta \in \mathcal{P}$.
Following the discussion provided immediately above, note that the robust performance case is conservative by definition, given that it optimises for the worst-case scenario, in terms of the (defined) system uncertainty. If an accurate nominal WEC model is available, then the (nominal) moment-based solution, presented in Section V-A, is more appropriate, since it delivers optimal results for Σ^0, and can be computed independent of the definition of the uncertainty set. On the other hand, if the presence of uncertainty is known to be significant, then the robust approach is preferred, given that it 'alleviates' the potential drop in performance arising from not having an accurate WEC model, by optimising for the worst-case (uncertainty) scenario.

VII. Receding horizon solutions

Though highly computationally efficient, a standing assumption for the moment-based control strategies, presented in Sections V and VI, is that the wave excitation input f_e can be characterised by a T_0-*periodic* mapping, with $T_0 = 2\pi/\omega_0$, where ω_0 is the fundamental frequency. If the wave excitation estimation and forecasting requirements are introduced to the optimal control formulation, then this assumption can be limiting in practice. To alleviate the effect behind this periodicity assumption, a *receding-horizon* framework has been presented in [24], which introduces a simple modification to the representation of the wave excitation signal in the moment-domain, as discussed below.

We begin by noting that, if T_0 is considered to be sufficiently large (*i.e.* ω_0 is sufficiently small) then the wave excitation input can be effectively considered T_0-periodic, for any practical purposes (see [42]). Nonetheless, this remark poses a contradiction: While the moment-based controllers, recalled in Sections V and VI, would require a sufficiently large time T_0 (equivalent to a sufficiently large time-horizon in (8)), state-of-the-art forecasting algorithms are not usually able to provide an accurate prediction of the wave excitation force for more than a couple of seconds [31], *i.e.* precise information is available throughout a shorter time T_h.

Motivated by this limitation in terms of implementation, [24] introduces a modification of the representation of f_e in the moment-domain, suitable for receding-horizon control, as follows. Suppose $\tilde{f}_{e_N}$ denotes the approximated wave excitation input for a given time-window Ξ_N, composed of *both* estimated and forecasted values (see Fig. 6). Using the underlying philosophy of the *short-term Fourier transform* [46], the so-called *apodised* wave excitation input can be written as $\lfloor \tilde{f}_{e_N} \rfloor_\vartheta = \vartheta \tilde{f}_{e_N}$, where the *apodisation* (often also called *windowing*) mapping $\vartheta : \Xi_N \times \mathbb{R}^+ \to [0\ 1]$ is used to smoothly bring the wave excitation signal, defined for a time-horizon T_h, down to zero at the edges of the set Ξ_N. In other words, the apodised signal $\lfloor \tilde{f}_{e_N} \rfloor_\vartheta$ is smoothly brought to zero at the boundaries so that the derivative of its periodic extension is sufficiently smooth, hence now being well-represented by a signal generator of the form (2) (as in Sections V and VI).

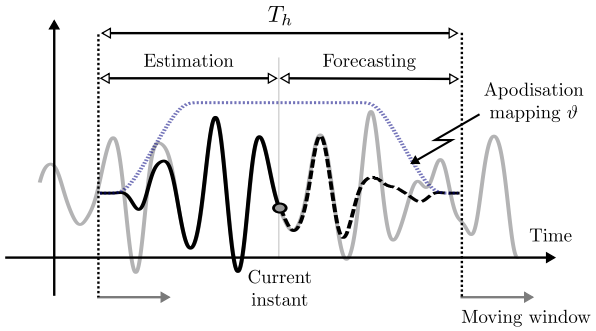

Fig. 6: Target excitation f_{e_N} (solid grey), and (apodised) approximated wave excitation input $\lfloor \tilde{f}_{e_N} \rfloor_\vartheta$ (black), for the time-window Ξ_N. Fig. adapted from [24].

With the apodised wave excitation estimate, the control problem is then solved for the time window Ξ_N, the computed optimal input is applied for a time $\Delta T_h \in \Xi_N$, and the window is shifted so as to repeat the process, *i.e.* in a receding-horizon fashion.

Remark 11: The receding-horizon moment-based controller [24] requires the addition of initial and terminal (equality) constraints to either (9) (linear WEC) or (10) (nonlinear WEC). The former guarantee consistency with respect to the measured outputs of the WEC system, while the latter enforces closed-loop stability.

VIII. Illustrative design example

To demonstrate the performance of the moment-based control framework, we consider the application

of a receding-horizon nonlinear controller to a full-scale state-of-the-art CorPower-like wave energy device oscillating in heave (translational motion). This device, whose dimensions are based on the experimental study performed in [47], and has been also considered in [14] for (open-loop) nonlinear moment-based control. We consider herein waves generated stochastically from a JONSWAP spectrum, with $\bar{H}_s = 2$ [m], $\bar{T}_p \in [5, 12]$ [s], $\gamma = 3.3$, and a length of $T = 230$ [s].

We take into account two main nonlinear hydrodynamic forces: viscous effects, and nonlinear restoring forces. Viscous effects are included via a Morison-like term, *i.e.* $\mathcal{F}_v(\dot{x}) = -\beta_v|\dot{x}|\dot{x}$, where $\beta_v = \frac{1}{2}\rho\gamma_d D$, $\gamma_d \in \mathbb{R}^+$ is the so-called drag coefficient, ρ is the water density, and D is the characteristic area of the device. The drag coefficient is set to $\gamma_d = 0.35$, based on the analysis performed in [48]. Nonlinear restoring effects are characterised based on the experimental results presented in [47]. In particular the following mapping $\mathcal{F}_r^{nl}(x) = \beta_{r_1}x^2 + \beta_{r_2}x^3$ is considered, where the coefficients $\{\beta_{r_1}, \beta_{r_2}\} \subset \mathbb{R}$ are determined based on a least-squares fit, using the experimental results of [47] as target set, giving a final result of $\beta_{r_1} = -1.55 \times 10^4$ [kg/ms^2] and $\beta_{r_2} = 0.82 \times 10^4$ [kg/m^{2}s^2].

The receding time-horizon is set to $T_h = 30$ [s], *i.e.* we consider 15 [s] of both estimated and forecasted values of f_e. Note that this corresponds to a fundamental frequency (for a specific time window Ξ_N) of $\omega_0 = 2\pi/30$ [rad/s], which provides an accurate representation of the (windowed) excitation force in terms of an implicit signal generator (*i.e.* as in (2)). The receding window is shifted every 0.1 [s], corresponding with a sampling rate of 10 [Hz]. The order of the *extended* signal generator, used to approximate the corresponding nonlinear moment to then solve the energy-maximising OCP (see Section V-B), is set to $\bar{N}_h = 30$. Finally, we set the maximum allowed displacement and velocity values to $Z_{\max} = 2$ [m] and $\dot{Z}_{\max} = 2$ [m/s]. The resulting finite-dimensional NP is solved using a local interior point method, where we take explicit advantage of the strict outer convexity of the energy-related objective function when mapped to the moment-domain, to numerically ensure that the (potentially local) solution computed with interior-point methods is, effectively, a global energy-maximiser (see [14] for further detail).

We now present performance results for the receding-horizon nonlinear moment-based controller, under both displacement and velocity constraints, and we compare these (for the benefit of the reader) with the performance of its linear moment-based counterpart, where both viscous and nonlinear hydrodynamic effects are disregarded at the control design stage. Fig. 7 explicitly shows motion (displacement and velocity) of the device under optimal control conditions, driven by a particular input wave realisation, for both linear and nonlinear controllers. Furthermore, instantaneous power and cumulative energy are also shown, directly highlighting the difference between linear and nonlinear controllers in terms of energy absorption performance. Note that, though both controllers are effectively able to respect the constraint specifications, the linear controller does not fully capture the 'in-phase' condition (*i.e.* phase synchronization) with the wave excitation force input (see, for instance, [2]), since it ignores relevant nonlinear dynamics affecting the WEC at the design stage. This results in both a larger reactive power flow, and less energy absorption.

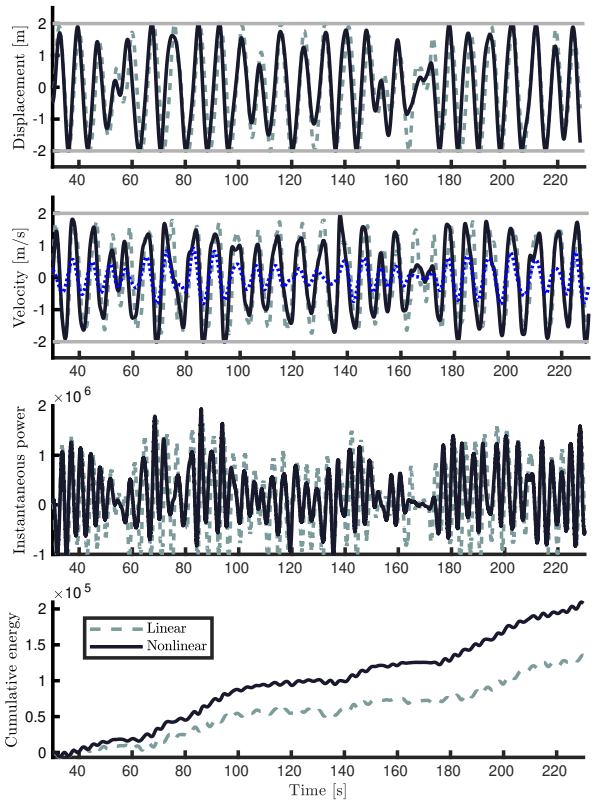

Fig. 7: Displacement, velocity, instantaneous power, and cumulative energy for an irregular wave realisation, for both linear (dashed-gray) and nonlinear (solid-black) moment-based controllers. The (scaled) wave excitation input is denoted using a dotted-blue line.

IX. Conclusions

The moment-domain presents an ideal framework for solving the WEC control, and related, problems. The choice of variable parameterisation, effected by the appropriate selection of signal generator in the moment-based framework results in computationally efficient solutions, permitting real-time implementation, even for arrays. The movement from linear to nonlinear representations, necessitated by the use of control action itself, is relatively smooth and, most importantly, both linear and nonlinear WEC control formulations present a convex optimisation problem, with corresponding uniqueness and ease of global solution.

References

[1] J. Ringwood, G. Bacelli, and F. Fusco, "Energy-maximizing control of wave-energy converters: The development of control system technology to optimize their operation," *IEEE Control Systems*, vol. 34, no. 5, pp. 30–55, 2014.

[2] D. García-Violini, N. Faedo, F. Jaramillo-Lopez, and J. V. Ringwood, "Simple controllers for wave energy devices compared," *Journal of Marine Science and Engineering*, vol. 8, no. 10, p. 793, 2020.

[3] N. Faedo, S. Olaya, and J. V. Ringwood, "Optimal control, mpc and mpc-like algorithms for wave energy systems: An overview," *IFAC Journal of Systems and Control*, vol. 1, pp. 37–56, 2017.

[4] N. Faedo, D. García-Violini, Y. Peña-Sanchez, and J. V. Ringwood, "Optimisation-vs. non-optimisation-based energy-maximising control for wave energy converters: A case study," in *European Control Conference (ECC)*. IEEE, 2020, pp. 843–848.

[5] A. Astolfi, "Model reduction by moment matching for linear and nonlinear systems," *IEEE Transactions on Automatic Control*, vol. 55, no. 10, pp. 2321–2336, 2010.

[6] A. Astolfi, G. Scarciotti, J. Simard, N. Faedo, and J. V. Ringwood, "Model reduction by moment matching: Beyond linearity a review of the last 10 years," in *59th IEEE Conference on Decision and Control (CDC)*. IEEE, 2020, pp. 1–16.

[7] J. Hals, J. Falnes, and T. Moan, "Constrained optimal control of a heaving buoy wave-energy converter," *Journal of Offshore Mechanics and Arctic Engineering*, vol. 133, no. 1, 2011.

[8] J. A. Cretel, G. Lightbody, G. P. Thomas, and A. W. Lewis, "Maximisation of energy capture by a wave-energy point absorber using model predictive control," *IFAC Proceedings Volumes*, vol. 44, no. 1, pp. 3714–3721, 2011.

[9] G. Bacelli and J. V. Ringwood, "Numerical optimal control of wave energy converters," *IEEE Transactions on Sustainable Energy*, vol. 6, no. 2, pp. 294–302, 2014.

[10] O. Abdelkhalik, R. Robinett, S. Zou, G. Bacelli, R. Coe, D. Bull, D. Wilson, and U. Korde, "On the control design of wave energy converters with wave prediction," *Journal of Ocean Engineering and Marine Energy*, vol. 2, no. 4, pp. 473–483, 2016.

[11] G. Li, "Nonlinear model predictive control of a wave energy converter based on differential flatness parameterisation," *International Journal of Control*, vol. 90, no. 1, pp. 68–77, 2017.

[12] N. Faedo, G. Scarciotti, A. Astolfi, and J. V. Ringwood, "On the approximation of moments for nonlinear systems," *IEEE Transactions on Automatic Control (Early access)*, 2021.

[13] ——, "Energy-maximising control of wave energy converters using a moment-domain representation," *Control Engineering Practice*, vol. 81, pp. 85–96, 2018.

[14] ——, "Nonlinear energy-maximizing optimal control of wave energy systems: A moment-based approach," *IEEE Transactions on Control Systems Technology (Early access)*, 2021.

[15] N. Faedo, Y. Peña-Sanchez, and J. V. Ringwood, "Finite-order hydrodynamic model determination for wave energy applications using moment-matching," *Ocean Engineering*, vol. 163, pp. 251–263, 2018.

[16] N. Faedo, Y. Pena-Sanchez, G. Giorgi, and J. V. Ringwood, "Moment-matching-based input-output parametric approximation for a multi-dof wec including hydrodynamic nonlinearities," in *13th European Wave and Tidal Energy Conference (EWTEC)*, 2019, pp. 1449–1.

[17] Y. Peña-Sanchez, N. Faedo, and J. V. Ringwood, "Moment-based parametric identification of arrays of wave energy converters," in *American Control Conference (ACC)*. IEEE, 2019, pp. 4785–4790.

[18] N. Faedo, Y. Peña-Sanchez, and J. V. Ringwood, "Parametric representation of arrays of wave energy converters for motion simulation and unknown input estimation: a moment-based approach," *Applied Ocean Research*, vol. 98, p. 102055, 2020.

[19] N. Faedo, F. J. D. Piuma, G. Giorgi, and J. V. Ringwood, "Nonlinear model reduction for wave energy systems: a moment-matching-based approach," *Nonlinear Dynamics*, vol. 102, no. 3, pp. 1215–1237, 2020.

[20] N. Faedo, D. García-Violini, G. Scarciotti, A. Astolfi, and J. V. Ringwood, "Robust moment-based energy-maximising optimal control of wave energy converters," in *IEEE 58th Conference on Decision and Control (CDC)*. IEEE, 2019, pp. 4286–4291.

[21] N. Faedo, G. Bracco, G. Mattiazzo, and J. V. Ringwood, "Robust energy-maximising control of wave energy systems under input uncertainty," in *IEEE 60th Conference on Decision and Control (CDC) (Under review)*. IEEE, 2021.

[22] N. Faedo, G. Scarciotti, A. Astolfi, and J. V. Ringwood, "Moment-based constrained optimal control of an array of wave energy converters," in *American Control Conference (ACC)*. IEEE, 2019, pp. 4797–4802.

[23] ——, "Energy-maximising moment-based constrained optimal control of ocean wave energy farms," *IET Renewable Power Generation (Under review)*, 2021.

[24] N. Faedo, Y. Peña-Sanchez, and J. V. Ringwood, "Receding-horizon energy-maximising optimal control of wave energy systems based on moments," *IEEE Transactions on Sustainable Energy*, vol. 12, no. 1, pp. 378–386, 2020.

[25] A. Day, A. Babarit, A. Fontaine, Y.-P. He, M. Kraskowski, M. Murai, I. Penesis, F. Salvatore, and H.-K. Shin, "Hydrodynamic modelling of marine renewable energy devices: A state of the art review," *Ocean Engineering*, vol. 108, pp. 46–69, 2015.

[26] L. Papillon, R. Costello, and J. V. Ringwood, "Boundary element and integral methods in potential flow theory: a review with a focus on wave energy applications," *Journal of Ocean Engineering and Marine Energy*, pp. 1–35, 2020.

[27] C. Windt, J. Davidson, and J. V. Ringwood, "High-fidelity numerical modelling of ocean wave energy systems: A review of computational fluid dynamics-based numerical wave tanks," *Renewable and Sustainable Energy Reviews*, vol. 93, pp. 610–630, 2018.

[28] J. M. Domínguez, A. J. Crespo, M. Hall, C. Altomare, M. Wu, V. Stratigaki, P. Troch, L. Cappietti, and M. Gómez-Gesteira, "Sph simulation of floating structures with moorings," *Coastal Engineering*, vol. 153, p. 103560, 2019.

[29] M. Farajvand, D. Garcia-Violini, V. Grazioso, C. Windt, and J. Ringwood, "Quantifying hydrodynamic model uncertaintyfor robust control of wave energy devices," in *European Wave and Tidal Energy Conference (EWTEC), Plymouth*, 2021.

[30] Y. Peña-Sanchez, C. Windt, J. Davidson, and J. V. Ringwood, "A critical comparison of excitation force estimators for wave-energy devices," *IEEE Transactions on Control Systems Technology*, vol. 28, no. 6, pp. 2263–2275, 2019.

[31] Y. Pena-Sanchez, M. Garcia-Abril, F. Paparella, and J. V. Ringwood, "Estimation and forecasting of excitation force for arrays of wave energy devices," *IEEE Transactions on Sustainable Energy*, vol. 9, no. 4, pp. 1672–1680, 2018.

[32] J. Cunningham, N. Faedo, and J. V. Ringwood, "Excitation force estimation for wave energy systems using a moment-domain representation," in *European Wave and Tidal Energy Conference (EWTEC), Naples*, 2019, pp. 1449–1.

[33] C. Windt, N. Faedo, M. Penalba, F. Dias, and J. V. Ringwood, "Reactive control of wave energy devices–the modelling paradox," *Applied Ocean Research*, vol. 109, p. 102574, 2021.

[34] G. Giorgi, M. Penalba, and J. Ringwood, "Nonlinear hydrodynamic models for heaving buoy wave energy converters," in *Proc. Asian Wave and Tidal Energy Conference (AWTEC), Singapore*, 2016, pp. 144–153.

[35] G. Scarciotti and A. Astolfi, "Data-driven model reduction by moment matching for linear and nonlinear systems," *Automatica*, vol. 79, pp. 340–351, 2017.

[36] N. Faedo, "Optimal control and model reduction for wave energy systems: A moment-based approach," Ph.D. dissertation, Department of Electronic Engineering, Maynooth University, 2020.

[37] J. Falnes and A. Kurniawan, *Ocean Waves And Oscillating Systems: Linear Interactions Including Wave-Energy Extraction*. Cambridge University Press, 2020, vol. 8.

[38] Y. Pena-Sanchez, N. Faedo, J. V. Ringwood *et al.*, "A critical comparison between parametric approximation methods for radiation forces in wave energy systems," in *29th International Ocean and Polar Engineering Conference (ISOPE)*. International Society of Offshore and Polar Engineers, 2019.

[39] N. Faedo, Y. Peña-Sanchez, and J. V. Ringwood, "Passivity preserving moment-based finite-order hydrodynamic model identification for wave energy applications," *Advances in Renewable Energies Offshore (RENEW)*, vol. 2018, pp. 351–359, 2018.

[40] M. Mekhiche and K. A. Edwards, "Ocean power technologies powebuoy: System-level design, development and validation methodology," in *2nd Marine Energy Technology Symposium (METS)*, 2014, pp. 1–9.

[41] S. Boyd and L. Vandenberghe, *Convex optimization*. Cambridge university press, 2004.

[42] A. Mérigaud and J. V. Ringwood, "Free-surface time-series generation for wave energy applications," *IEEE Journal of Oceanic Engineering*, vol. 43, no. 1, pp. 19–35, 2018.

[43] H. X. Phu, "Outer γ-convexity in vector spaces," *Numerical Functional Analysis and Optimization*, vol. 29, no. 7-8, pp. 835–854, 2008.

[44] G. Giorgi and J. V. Ringwood, "Consistency of viscous drag identification tests for wave energy applications," in *12th European Wave and Tidal Energy Conference (EWTEC)*, 2017.

[45] A. Ben-Tal and A. Nemirovski, "Robust convex optimization," *Mathematics of operations research*, vol. 23, no. 4, pp. 769–805, 1998.

[46] K. M. Prabhu, *Window functions and their applications in signal processing*. CRC press, 2013.

[47] J. Hals, G. S. Ásgeirsson, E. Hjálmarsson, J. Maillet, P. Möller, P. Pires, M. Guérinel, and M. Lopes, "Tank testing of an inherently phase-controlled wave energy converter," *International Journal of Marine Energy*, vol. 15, pp. 68–84, 2016.

[48] G. Giorgi and J. V. Ringwood, "A compact 6-dof nonlinear wave energy device model for power assessment and control investigations," *IEEE Transactions on Sustainable Energy*, vol. 10, no. 1, pp. 119–126, 2018.